Dynamics of a Slung Load

L. Feaster,* C. Poli,† and R. Kirchhoff‡
University of Massachusetts, Amherst, Mass.

The yaw damping coefficient of an 8×8×20 ft cargo container is experimentally determined by forced oscillation tests. The result is then used in linearized small-perturbation stability analyses of a slung load, considering both single-cable and two-cable tandem suspension systems. The effect of attaching stabilizing fins to the container and of incorporating a rotating wheel for stability augmentation is also theoretically investigated. The results agree well with previous model and full-scale tests and also show that the two-cable tandem suspension system may offer a satisfactory means of transporting the standard cargo container throughout the speed range of most present-day cargo helicopters.

Nomenclature

b, S	=characteristic length and frontal area of towed body/model
K_1, K_2	=arbitrary amplitudes of forced oscillation
T	=cable force
U_0	=x component of steady-state velocity
u, v, w	=linear perturbation velocities
$X, Y, Z; L, M, N$	=aerodynamic forces; aerodynamic moments
X_u, X_w, etc.	=changes in aerodynamic forces and moments due to changes in velocities
x', y', z'	=linear perturbation displacements
α, β	=angle of attack and sideslip, respectively
β_1, β_2	=nondimensional parameters: $\beta_1 = K_1\omega/U_0$, $\beta_2 = (b\omega/2U_0)\beta_1$
θ, ϕ, ψ	=aircraft Euler angles
ρ	=free-stream density
ω	=frequency of forced oscillation
ω_ℓ	=wheel rotational speed
C_D, C_L, etc.	=conventional aerodynamic coefficients (Ref. 11)
$C_{L_\alpha}, C_{m_\alpha}$, etc.	$=\partial C_L/\partial\alpha, \partial C_m/\partial\alpha$, etc.
C_{n_β}	$=\partial C_n/\partial\beta = \left(\frac{\partial N}{\partial\beta}\right)\frac{2}{\rho U_0^2 Sb}$
$C_{n_{\dot\beta}}$	$=\partial C_n/\partial\dot\beta = \left(\frac{\partial N}{\partial\dot\beta}\right)\frac{4}{\rho U_0 Sb^2}$
C_{n_r}	$=\partial C_n/\partial\dot\psi = \left(\frac{\partial N}{\partial\dot\psi}\right)\frac{4}{\rho U_0 Sb^2}, r=\dot\psi$
$C_{n_{\ddot\psi}}$	$=\partial C_n/\partial\ddot\psi = \left(\frac{\partial N}{\partial\ddot\psi}\right)\frac{8}{\rho Sb^3}$

Introduction

THE subject or airborne towing has been one of continued interest over the past half century, and its applications have ranged from the towing of aerial gliders to the towing of underwater bodies for antisubmarine warfare. One need hardly mention the possible benefits available through helicopter sling load operations in remote-area construction, ship-to-shore port operations, and special construction applications. The development of the heavy-lift helicopter for the primary purpose of transporting external loads is one of the more recent trends to specialize the use of the helicopter for this purpose.

While almost any cargo can be carried externally if it is within the helicopter's payload capability, experience has shown that the operational envelope of the aircraft must frequently be restricted. That is, airspeeds are limited, complicated rigging methods are employed, and special stabilizing devices such as drag chutes or fins are used. Even with these precautions, instances still occur where the cargo must be jettisoned or the aircraft and crew endangered due to the instability of the load.

With the increased importance of airborne towing, several valuable investigations have been conducted in the area. Of the more recent works, Poli and Cromack[1] analyzed the stability of an 8×8×20 ft cargo container towed by a single cable attached at the center of gravity. Their analytical work, which was supplemented by static wind-tunnel tests, predicted a high-speed stable region and identified the drag-to-weight ratio of the slung load, D/W, and the length of the towing cable, ℓ, as significant stability parameters.

The results obtained by Poli and Cromack compare qualitatively with the earlier experimental work of Etkin and Mackworth.[2] Unlike Poli and Cromack, however, Etkin and Mackworth showed that an additional low-speed stable region could occur with favorable yaw damping.

Although the bulk of slung-load operations are currently being carried out with the UH-1 and CH-47 helicopters which are only equipped for single-point suspension, and in spite of the ease and speed of hookup and release and the uncomplicated and reliable jettison system, some researchers[3,5] have turned their attention to multi-cable suspension systems for heavier loads. This has been done because of the stability

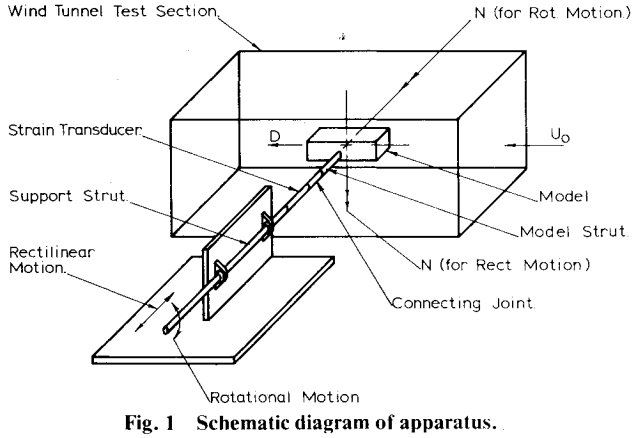

Fig. 1 Schematic diagram of apparatus.

Received Aug. 7, 1975; revision received July 8, 1976.
Index categories: Air Transportation Systems; VTOL Handling, Stability, and Control.

*Lt. Col., U. S. Army.
†Professor, Department of Mechanical and Aerospace Engineering.
‡Associate Professor, Department of Mechanical and Aerospace Engineering.

difficulties encountered using a single-point suspension system.

Other methods have also been studied to actively stabilize externally transported loads. Poli and Cromack[1] demonstrated that by the addition of fins there is an appreciable reduction in the length of single cables required for stability. Micale and Poli[6] investigated the possibility of gyroscopically stabilizing a rectangular cargo container towed with a single cable by incorporating a reaction wheel. An alternate method, using winches as active load controller, has been proposed by Asseo.[7-9]

The foregoing brief review, along with a study of the more extensive review provided by Sheldon,[10] indicates that previous research has provided a substantial body of information regarding the stability of slung loads. These investigations, however, have tended to be either qualitative in nature, reporting flight test and wind-tunnel results,[2-10] or the analytical treatment has been restricted by the difficulty of predicting C_{n_r}, the yaw damping coefficient.[1,6]

At present, there are no known analytical methods for accurately determining the yaw damping coefficient of a bluff body. Therefore, this study first experimentally determined the value of C_{n_r} for a box-shaped container and then analytically investigated the effect of this coefficient on the stability of the slung load for both single-cable and tandem suspension systems, as well as for loads which incorporated either fins or a rotating wheel for stability augmentation.

Wind-Tunnel Testing

For the wind-tunnel tests, a 1/27 scale styrofoam model was fabricated to represent an $8\times8\times20$ ft cargo container. The University of Massachusetts, Amherst, subsonic wind tunnel with a test section $20\times28\times36$ in. long was used for all tests. During the first phase of testing, the model was inserted in the test section on the end of a cantilever rod and forced to translate perpendicular to the airflow (Fig. 1) Sinusoidal rectilinear motion was obtained by using a vibration shaker to drive the support strut.

Expressing the linear velocity of the model

$$\dot{y}=K_1\omega\cos\omega t \tag{1}$$

where K_1 and ω are the amplitude and frequency of the forced oscillation, the linearized Taylor expansion of the aerodynamic moment, N, can be written as[10]

$$N=N_0+\left(\frac{\partial N}{\partial\beta}\right)\beta+\left(\frac{\partial N}{\partial\dot{\beta}}\right)\dot{\beta} \tag{2}$$

or, in dimensionless form

$$C_n=C_{n_\beta}+C_{n_{\dot\beta}}\left(\frac{d\beta}{d\tau}\right) \tag{3}$$

where $\beta=K_1\omega/U_0\cos\omega t$ is the effective sideslip angle; U_0 is the free-stream velocity; $\tau=2tU_0/b$ is the dimensionless time; b is the model length; C_n, C_{n_β}, and $C_{n_{\dot\beta}}$ are the aerodynamic coefficients as defined in the Nomenclature; and use was made of the fact that, for a symmetrical body, $\beta_0=\dot\beta_0=0$ implies $N_0=0$. Thus, if N is measured with respect to model displacement, y, the coefficients of Eq. (3) can be identified as the in-phase and out-of-phase components.

A strain transducer mounted on the support strut to sense the vector sum of the aerodynamic moment and the moment due to drag provided an input signal to a two-phase lock-in amplifier (LIA). The linear displacement of the model was used as the reference signal. Since the drag varied at twice the frequency of model displacement and because of the coherent rejection feature of the LIA, only the aerodynamic moment, N was measured. The LIA output then yielded the two aerodynamic coefficients in Eq. (3).

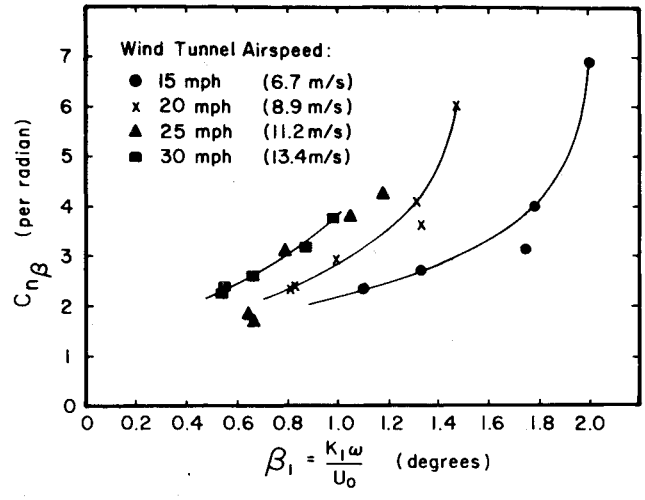

Fig. 2 Sinusoidal translation test results of the stability derivative, C_{n_β}, vs the dimensionless parameter, β_1.

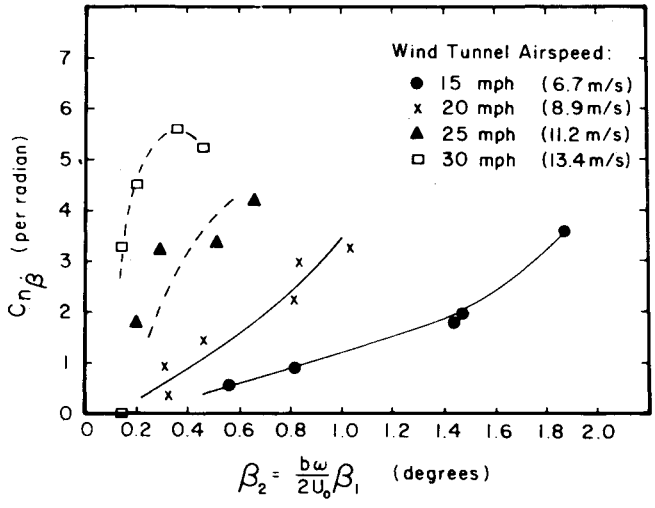

Fig. 3 Sinusoidal translation test results of the stability derivative, $C_{n_{\dot\beta}}$, vs the dimensionless parameter, β_2.

The values obtained for C_{n_β} as a function of the amplitude of dimensionless sideslip angle, $\beta_1=K_1\omega/U_0$, are shown in Fig. 2, while in Fig. 3 the values of $C_{n_{\dot\beta}}$ are given as a function of the dimensionless parameter, β_2. Since the expressions in Eq. (3) are to be evaluated at the steady-state condition, $\beta_0=\dot\beta_0=0$, the curves in Figs. 2 and 3 were analyzed in the limit as $\omega\to0$ with the results: $C_{n_\beta}\simeq1.0$/rad and $C_{n_{\dot\beta}}\simeq0$/rad. Here the extrapolation for C_{n_β} was further than desired, primarily due to the limitations of the testing apparatus. The results were accepted as reasonably valid, however, in view of the previously determined result[1] that $C_{n_\beta}=0.67$/rad and the knowledge that $C_{n_{\dot\beta}}$ could be expected to equal zero (no interference effects).

In the second phase of testing, sinusoidal rotary motion about the yaw axis was provided by driving a bellcrank attached to the support strut (Fig. 1). Initial tests were made using the vibration shaker; however, the drive mechanism was later modified to use a variable-speed, electric motor to test at very low frequencies. A torsional strain transducer furnished an input signal to a two-phase LIA, and the angular displacement of the model was used as the reference signal.

With the angular velocity of the model, $\dot\psi$, given by

$$\dot\psi=K_2\omega\cos\omega t \tag{4}$$

and noting that $\psi = -\beta$, the linearized expansion of the aerodynamic moment yields [10]

$$N = \frac{\partial N}{\partial \beta}\beta + \frac{\partial N}{\partial \dot{\beta}}\dot{\beta} + \frac{\partial N}{\partial \dot{\psi}}\dot{\psi} \frac{\partial N}{\partial \ddot{\psi}}\ddot{\psi} \tag{5}$$

or

$$C_n = C_{n_\beta}\beta + C_{n_{\dot{\beta}}}\left(\frac{d\beta}{d\tau}\right) - C_{n_r}\left(\frac{d\beta}{d\tau}\right) - C_{n_{\ddot{\psi}}}\left(\frac{d^2\beta}{d\tau^2}\right) \tag{6}$$

where β is the sideslip angle, $\beta = -\psi = -K_2 \sin\omega t$; C_{n_r} and $C_{n_{\ddot{\psi}}}$ are the aerodynamic coefficients as defined in the Nomenclature; and the remaining symbols have been previously defined. Again, if the aerodynamic moment, N, is determined as a vector measured with respect to the angular displacement of the body, the coefficients of Eq. (6) are given as the in-phase and out-of-phase components.

Although desirable, no electro-mechanical scheme was devised to cancel the effect of model inertia from the strain transducer output; thus, Eq. (5) could not be applied directly. Accordingly, from the rotational equation of motion for the model, the moment sensed by the strain transducer, $-M_T$, is given by

$$-M_T = N - C\ddot{\psi} \tag{7}$$

where C is the mass moment of inertia of the model about the rotational axis.

Combining Eqs. (5) and (7) and expressing the partial derivatives in dimensionless form, the in-phase component (IPC) becomes

$$\text{IPC} = \left[-C_{n_\beta}\frac{\rho U_0^2 Sb}{2} - C_{n_{\ddot{\psi}}}\frac{\rho Sb^3}{8}\omega^2 + C\omega^2 \right] K_2 \tag{8}$$

where ρ is the free-stream density and S the frontal area of the model. Considering two test conditions where the only variable is wind-tunnel velocity, U_0, Eq. (8) may be written for each condition and the resulting equations subtracted to yield, after rearranging terms

$$C_{n_\beta} = -[(\text{IPC})_2 - (\text{IPC})_1]\frac{2}{\rho SbK_2(U_{02}^2 - U_{01}^2)} \tag{9}$$

A similar development for the out-of-phase component (OPC) shows

$$C_{n_r} - C_{n_{\dot{\beta}}} = [(\text{OPC})_2 - (\text{OPC})_1]\frac{4}{\rho Sb^2 K_2 \omega (U_{02} - U_{01})} \tag{10}$$

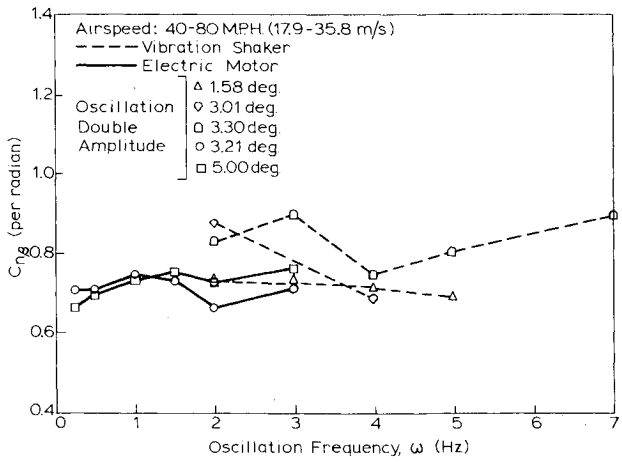

Fig. 4 Sinusoidal translation test results of the stability derivative, C_{n_β}, vs oscillation frequency, ω.

Figure 4 shows the results obtained for C_{n_β} as a function of frequency. The results obtained using the electric motor show little scatter and are essentially independent of frequency—a result predicted from the theory. An approximate value of C_{n_β} from these curves is 0.7/rad, where the correlation with Ref. 1 is very good.

The values obtained for the damping term, $[C_{n_r} - C_{n_{\dot{\beta}}}]$, at constant oscillation double amplitudes are shown in Fig. 5. As seen from this figure, the values of $[C_{n_r} - C_{n_{\dot{\beta}}}]$ determined from both phases of testing (vibration shaker and electric motor) tend to change sign from minus to plus at oscillation frequencies above 2 Hz. For frequencies below 2 Hz, the term reaches a maximum negative (stabilizing) value near 1 Hz and then tends toward a very small negative value (0 to −0.3/rad) as the oscillation frequency approaches zero.

Based on the above experiments, it is concluded that

$$-0.3 < C_{n_r} < 0/\text{rad} \tag{11}$$

since the value is desired in the limit as $\omega \to 0$ (i.e., $\dot{\psi} \to 0$).

Stability Analyses

The results of the previous section are now used in linearized small-perturbation stability analyses of a slung load considering both single-cable and two-cable tandem suspension systems. The effect of attaching stabilizing fins to the container and of incorporating a rotating wheel for stability augmentation is also investigated.

Container weights chosen for the analyses correspond to the approximate maximum load carried externally by current generation helicopters (4,000-10,000 lb) and to the weight of an empty container (2,000 lb).

Single-Cable Suspension

The linearized equations of motion for a rigid body being towed by a single cable beneath a helicopter flying at constant velocity, U_0, (Fig. 6) are derived in Ref. 1. It was assumed in that derivation that the towing craft was flying straight and level, that the aerodynamic forces and moments of the slung load were such that the lateral and longitudinal degrees of freedom were uncoupled, that the load was outside the wake of the helicopter rotor, that the rigid body motion of the load was uncoupled from the dynamical motion of the cable, and lastly that $C_{n_r} = C_{m_q} = 0$.

If the yaw damping stability derivative, N_r, and the pitch damping stability derivative, M_q, are included in the linearized equations of motion of Ref. 1, it can be shown [11] that the necessary and sufficient condition for lateral stability is

$$\begin{aligned} &a^2\{bC_{n_\beta}[-CmC_{n_\beta}(C_{y_\beta} + C_D) \\ &-(C_{n_r}/2)(C\rho SbC_{y_\beta}^2/2 + b^2m^2C_{n_\beta} + \rho Sb^3mC_{n_r}C_{y_\beta}/4)]\} \\ &+a[-C^2C_{y_\beta}C_{n_\beta}(C_{y_\beta} + C_D) - (b^2C_{n_r}/2)(CmC_{n_\beta}C_{y_\beta} \\ &-C\rho SbC_{n_r}C_{y_\beta}^2/4 - CmC_{n_\beta}C_D - \rho Sb^3mC_{n_r}^2C_{y_\beta}/8)] \\ &+(C^2bC_{y_\beta}C_{n_r}C_D/2) > 0 \end{aligned} \tag{12}$$

where m is the mass of the towed body; a and h are the horizontal and vertical distances between the cable attachment points; C is the moment of inertia of the towed body about the z axis; and the non-dimensional stability derivatives, C_{n_β}, C_{y_β}, etc., are defined in the Nomenclature.

Thus, the stability condition for the lateral mode reduces to a quadratic expression in the variable a. Since a is related to the cable length, ℓ, through the steady-state towing angle, γ, one may assume that Eq. (12) will normally produce two critical cable lengths providing the boundaries for three stability regions. As can be easily verified, Eq. (12) above reduces to Eq. (8) of Ref. 1 if $C_{n_r} = 0$.

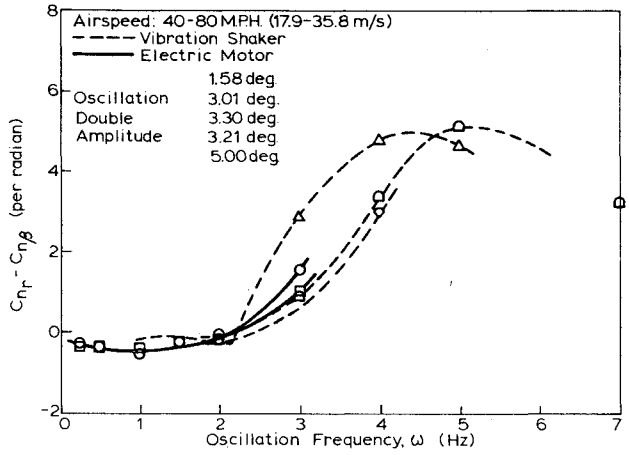

Fig. 5 Sinusoidal rotation test reuslts of the damping term, $C_{n_r} - C_{n_\beta}$, vs oscillation frequency, ω.

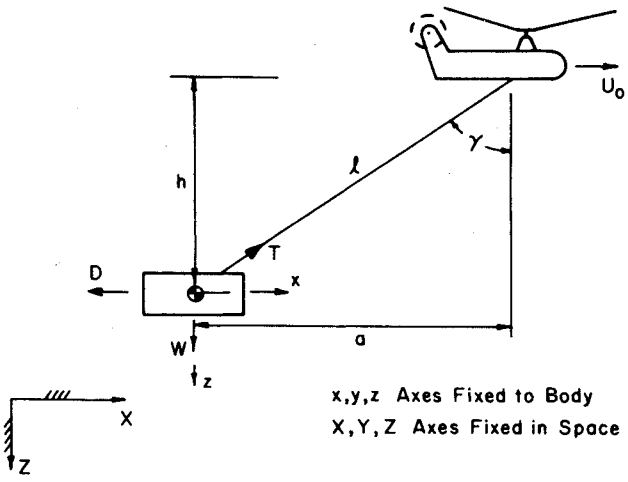

Fig. 6 Steady-state towing of a rigid body, single-cable suspension.

Using the static stability derivaties obtained by Poli and Cromack[1] (Table 1), the results of the lateral stability requirement, Eq. (12), for an $8 \times 8 \times 20$ ft container without stabilizing fins are presented in Fig. 7. A weak dependency on container weight was indicated in the solution of Eq. (12); however, this variation was within the plotting accuracy of the figure for weights between 5,000 and 30,000 lb.

It is interesting to note that the upper boundary of the unstable region in Fig. 7 does not shift position for different values of C_{n_r} within the given range. In fact, this boundary coincides with the results found by Poli and Cromack[1] where damping was neglected. The lower boundary does change, however, with the lower stable region increasing in size as C_{n_r} becomes more negative. In particular, the lower curve for $C_{n_r} = -0.30$/rad would indicate that a 5,000-lb container on a 15-ft cable should be stable to drag-to-weight ratios of .08 or airspeeds near 50 mph.[§] Since instabilities have occurred at lower airspeeds in actual flight test,[3] the true value of C_{n_r} is expected to be more positive than -0.30/rad.

For the container under investigation, $C_{m_q} = C_{n_r}$; therefore, the longitudinal stability was examined over the same range of values for the damping coefficient as was done in the lateral case. As in Ref. 1, the results[11] show that the lateral mode is the more critical; that is, a cable length and drag-to-weight ratio that ensure lateral stability also ensure longitudinal stability.

[§]Here the drag coefficient was taken as .915, in consonance with Ref. 1.

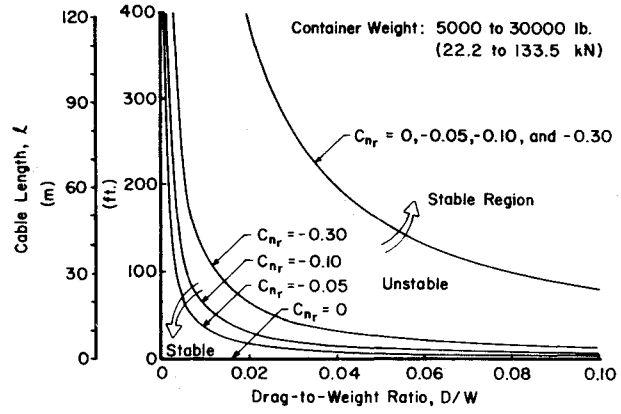

Fig. 7 Lateral stability of box without fins, single-cable suspension.

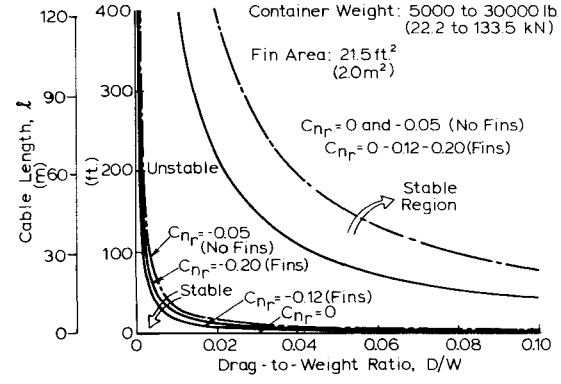

Fig. 8 Lateral stability of box with fins, single-cable suspe ision.

Figure 8 shows the effect on lateral stability of attaching stabilizing fins to the edges of the container in a crucifix pattern. The static aerodynamic data were again taken from the Poli-Cromack[1] investigation (Table 1); and the fin contribution to yaw damping was estimated[11,12] to be $-0.15 < C_{n_r} < -0.07$/rad. Thus, one set of stability boundaries was calculated with $C_{n_r} = -0.20$/rad where the body contribution was assumed equal to -0.05/rad; and a second, more conservative set of boundaries, was calculated with $C_{n_r} = -0.12$/rad. To show the effect of neglecting the damping term for a box with fins, a curve with $C_{n_r} = 0$ was plotted. For comparison, curves for a box without stabilizing fins ($C_{n_r} = 0$ and -0.05/rad) are also included in Fig. 8.

The results for a box with fins and damping neglected are again identical with those obtained in Ref. 1 and show that: 1) a single boundary is predicted for the lateral mode; and 2) above a drag-to-weight ratio, D/W, of 0.02 a reduction in cable length of nearly 40% is possible by adding fins. By including C_{n_r}, however, three stability regions appear for the lateral mode—two stable regions separated by an unstable region. From Fig. 8 it can be seen that the upper boundaries (with and without fins) remain unchanged for negative values of C_{n_r} and still show an improvement for a container with stabilizing fins. The lower boundaries, on the other hand, reveal that the lower stable region is more compressed for a box with fins. That is, for a box without fins, higher values of D/W (and thus higher airspeeds) can be attained for a given cable length than for a box with fins.

With $C_{m_q} = C_{n_r}$, the longitudinal mode for a box with fins was examined;[11] and again the lateral degrees of freedom presented the determining factor for stability.

The linearized equations of motion for a rigid body containing a rotating wheel and being towed by a single cable beneath an aircraft flying at constant velocity, U_0, are given in Ref. 6. In addition to the assumptions made previously, it was assumed that the center of mass of the box and wheel

Table 1 Stability derivaties[1] (in deg^{-1})

Configuration	C_{D_0}	C_{L_0}	C_{D_α}	C_{L_α}	C_{m_α}	C_{y_β}	C_{l_β}	C_{n_β}
Box-no fins	.915	0	0	.0317	−.0117	−.0477	0	.0117
Box-fins	.930	0	0	.0563	−.0325	−.0725	0	.0325
Fin area = 21.5 ft^2								

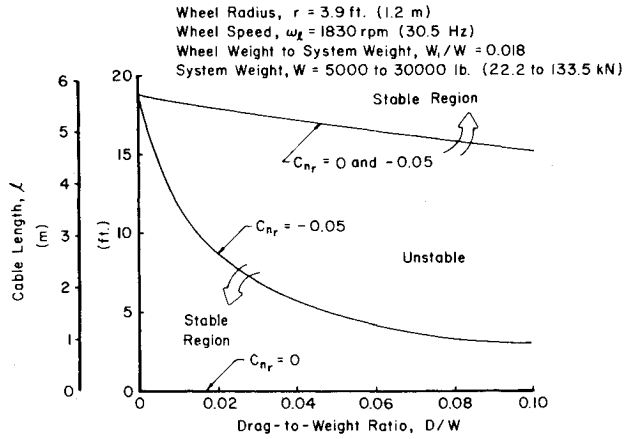

Fig. 9 Lateral stability of box with a rotating wheel, single-cable suspension.

coincided, that the rotating wheel was initially spun up, that the housing unit of the wheel and negligible mass and momentum, and that the friction in the wheel bearings was negligible.

If yaw damping, N_r, and pitch damping, M_q, are retained in these equations, the stability requirements[11] for $C_{n_r}=0$ and -0.05/rad are as shown in Fig. 9.

With $C_{n_r}=0$, the single boundary of Fig. 9 coincides with its counterpart in Ref. 6. For slightly stabilizing values of the damping coefficient ($C_{n_r}=-0.05$/rad), the upper boundary of the unstable region does not change position. At the same time, a lower boundary appears which defines a stable region for very short cable lengths. Comparison of Figs. 7 and 9 shows that a considerable reduction in cable length can be achieved by incorporating a rotating wheel. It should be noted, however, that any desirable consequences of the lower stable region depicted in Fig. 7 are nearly eliminated by the effect of the wheel. In this respect, the result of adding a rotating wheel is much the same as adding stabilizing fins.

The characteristic equation for the longitudinal mode was found to be identical with the one developed for a rigid body without a wheel.[11] Thus, the stability boundary shown in Refs. 1 and 6 is applicable with $C_{m_q}=0$. In the more likely event that C_{m_q} is slightly negative, it was determined that the longitudinal mode was stable for all practical cable lengths and for systems weights in the range discussed.

Here it is observed that, when damping was neglected, Micale and Poli[6] concluded that the longitudinal mode would become the controlling factor for a box with a rotating wheel. On the other hand, the current analysis shows that for small negative values of pitch damping, the longitudinal mode is stable and the lateral degrees of freedom remain critical. It is suggested, therefore, that the cable length can be decreased to almost any suitable length by proper choice of wheel size and speed and that these quantities themselves represent the practical controlling factor.

Two-Cable Tandem Suspension

The linearized equations of motion for a rigid body suspended by two longitudinally displaced cables and being towed beneath an aircraft flying at constant velocity, U_0, (Fig. 10) are developed in Ref. 11. For ease of analysis, the case of two parallel cables of equal length, ℓ, with equidistant attachment points from the center of gravity of the rigid body is considered.

The assumptions made in the derivation of the mathematical model were the same as those used in the single-cable case. The equations of motion are

Lateral:

$$\begin{bmatrix} (m\lambda - Y_v) & \left[mU_0\lambda - \frac{X_0}{h}(h+d_2)\right] & -d_2X_0/a & -X_0/a \\ -L_v & -d_2\frac{X_0}{h}(h+d_2) & \left[A\lambda^2 - d_2\frac{X_0}{a}(h+d_2)\right] & -d_2X_0/a \\ -N_v & \left[C\lambda^2 - N_r\lambda - X_0\left(\frac{d_1^2}{a}\right) + d_2\left(\frac{a}{h}\right)\right] & -d_2\frac{X_0}{h}(h+d_2) & -d_2X_0/h \\ 1 & U_0 & 0 & -\lambda \end{bmatrix} \begin{bmatrix} v \\ \psi \\ \phi \\ y' \end{bmatrix} = 0 \tag{13}$$

Longitudinal:

$$\begin{bmatrix} (m\lambda - X_u) & -X_w & -a/\ell & -a/\ell & -X_0/a & 0 \\ -Z_u & (m\lambda - Z_w) & h/\ell & h/\ell & 0 & -X_0/a \\ -M_u & -M_w & -\left(d_1\frac{h}{\ell} - d_2\frac{a}{\ell}\right) & \left(d_1\frac{h}{\ell} + d_2\frac{a}{\ell}\right) & -d_2X_0/a & d_2X_0/h \\ -1 & 0 & 0 & 0 & \lambda & 0 \\ 0 & -1 & 0 & 0 & 0 & \lambda \\ 0 & 0 & 0 & 0 & -a & h \end{bmatrix} \begin{bmatrix} u \\ w \\ \Delta T_1 \\ \Delta T_2 \\ x' \\ z' \end{bmatrix} = 0 \tag{14}$$

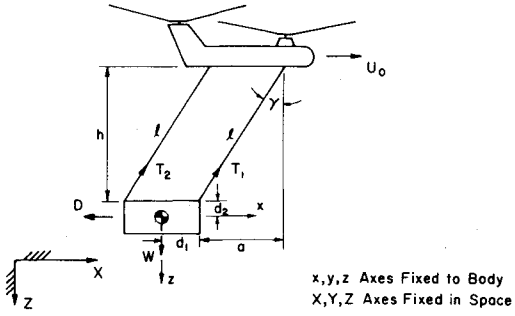

Fig. 10 Steady-state towing of a rigid body, two-cable tandem suspension.

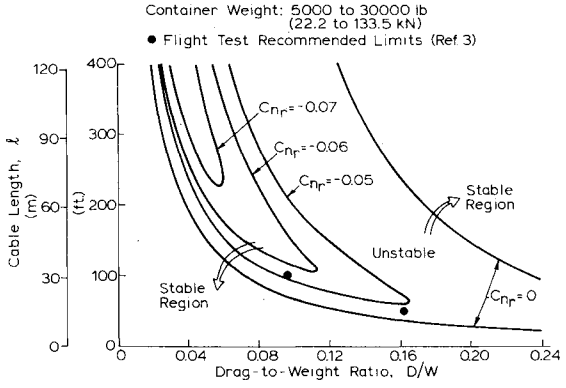

Fig. 11 Lateral stability of box without fins, two-cable tandem suspension.

where $\lambda = d/dt$; and d_1 and d_2 locate the cable attachment points along the x and z axes, respectively; where A, B, and C represent the moments of inertia of the towed body about the x, y, and z axes, respectively; u, v, and w represent the linear perturbation velocities along x, y, and z, respectively; θ, ψ, and ϕ are the angles of pitch, yaw, and roll, respectively; x',y', and z' are the linear displacements of the center of mass of the towed body from steady-state flight; X, Y, Z, L, M, and N are the aerodynamic forces and moments along x, y, and z, respectively; X_u, Y_v, etc. are the changes in the aerodynamic forces and moments due to changes in the linear and angular velocities; and ΔT is the change in the cable tension from its steady-state value.

To analyze the stability of the lateral and longitudinal motions of the towed body, the determinant of coefficients in Eqs. (13) and (14) must be expanded to obtain the characteristic equations. The Routh Hurwitz criteria may then be applied to the characteristic equations to determine the stability of each mode. Finally, it should be recalled that for the container being studied, the results of Ref. 1 show that at the equilibrium position of $\alpha = \beta = 0$, $Z_0 = Z_u = X_w = M_u = L_v = 0$.

For the lateral degrees of freedom, the above procedures were considered overly burdensome and susceptible to error for manual manipulation; thus, they were evaluated using an APL computer program.

The results for a standard cargo container without stabilizing fins are presented in Fig. 11. The cables were assumed to be attached to the ends of the box at the upper corners as shown in Fig. 10. Curves are shown for $C_{n_r} = 0$, -0.05, -0.06, and -0.07/rad. For values of C_{n_r} more negative than -0.07/rad, no instability was predicted for cable lengths less than 400 ft. A weak dependency on container weight was indicated in the computer solution; but, as before, the variation was within the plotting accuracy of the figure for the weights considered.

Here it was of interest to compare the results of flight testing with the stability boundaries just presented. For flight-test conditions which very closely matched the assumptions of the current investigation, a qualitative report by Hutto[3] was found useful. For level flight with 50- and 100-ft cables, Hutto recommended maximum airspeeds of 65 and 50 knots, respectively, where both limit airspeeds were determined by a yawing oscillation of the container. Using the drag coefficient from Ref. 1, the drag-to-weight ratios for the above airspeeds were determined and the values of cable length plotted in Fig. 11. As seen from the figure, the predicted stability boundary with $C_{n_r} = -0.05$/rad offers a very good fit to the two points obtained from flight test information.

Expansion of the determinant of coefficients in Eq. (14) for the longitudinal mode is simplified by the numerous zero elements. It may easily be found that the characteristic equation is a quadratic in λ and that, for the box-shaped container being studied, the coefficients are all positive. Thus, the conditions for stability are automatically satisfied.

As may have been expected, the lateral mode is the controlling factor in determining stability, and the longitudinal mode may be neglected. The symmetric degrees of freedom do, however, define the limiting case of the aft cable becoming slack. With reference to Fig. 10, the equilibrium conditions prescribe that this situation occurs when $0 < D/W < d_1/d_2$. For the container and suspension system being considered, this relation becomes $0 < D/W < 2.5$, which indicated an airspeed well beyond the maximum of current cargo helicopters.

The change in stability caused by attaching stabilizing fins to the container is examined for the two-cable system in Ref. 11. The results for the lateral mode are similar in appearance to Fig. 11; but, as occurred with single-cable suspension, the boundaries shift inward toward the origin. A favorable trend is indicated in that the upper boundries converge more rapidly to the horizontal axis, except that the unstable regions must first be traversed to reach the desired outer region of stability.

Overall, the effect on lateral stability when fins are attached is detrimental in that the maximum cable length for complete stability is decreased; and, for longer cables, the onset of instability takes place at lower values of the drag-to-weight ratio. As before, the longitudinal degrees of freedom are asymptotically stable, and the lateral mode is of primary concern.

If a rotating wheel is incorporated into the two-cable tandem system, the linearized equations of motion may be written by including the additional terms arising from the wheel.[6] None of these terms appear in the longitudinal equations[11] which are identical to Eq. (14); thus, the longitudinal mode is asymptotically stable for all cable lengths. The lateral equations, on the other hand, are given by Eq. (15), where the symbols have been previously defined.

Lateral:

$$\begin{bmatrix} (m_l\lambda - Y_v) & [m_l U_0\lambda - (X_0/h)(h+d_2)] & -d_2X_0/a & -X_0/a \\ -L_v & [-\lambda\omega_l C_l - (d_2X_0/h)(h+d_2)] & [(A+A_l)\lambda^2 - (d_2X_0/h)(h+d_2)] & -d_2X_0/a \\ -N_v & [(C+A_l)\lambda^2 - N_r\lambda - X_0(d_1^2/a + d_2a/h)] & [\lambda\omega_l C_l - (d_2X_0/h)(h+d_2)] & -d_2X_0/h \\ l & U_0 & 0 & -\lambda \end{bmatrix} \begin{bmatrix} v \\ \psi \\ \phi \\ y' \end{bmatrix} = 0 \quad (15)$$

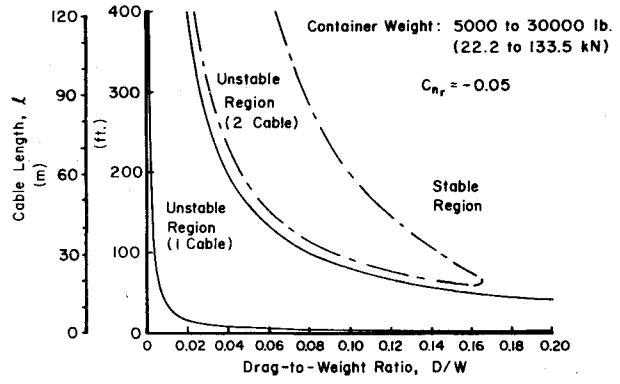

Fig. 12 Summary plot of lateral stability of box without fins, single-cable and two-cable tandem suspension.

The assumption pertinent to the above equations are the same as those stated earlier for a rigid body suspended by a single cable and containing a rotating wheel. As in the previous cases, the spin axis of the wheel is aligned with the y body axis; and the two cables are assumed to be parallel, of equal length, ℓ, and to have equidistant attachment points from the center of gravity of the container.

To examine the stability of the lateral degrees of freedom, the determinant of coefficients in Eq. (15) was again expanded and the characteristic equation analyzed via the Routh Hurwitz criteria using computer techniques. The results, as presented in Ref. 11, show that the addition of a rotating wheel virtually eliminated the lower stable region found in Fig. 11. Additionally, the stability boundaries indicate a definite weight sensitiveness, with the size of the unstable region becoming larger as container weight increases. Unfortunately, even at the lighter system weight of 5,000 lb, cable lengths in excess of 100 ft are required for stable conditions at drag-to-weight ratios as low as $D/W = 0.05$.

Summary and Conclusions

The experimental portion of this investigation shows that the yaw damping coefficient, C_{n_r}, is within the range $-0.3 < C_{n_r} < 0$. In light of the comparisons made with flight-test observations, a more refined estimate may be taken as $C_{n_r} = -0.05$/rad. With this value the stability boundaries for both the single-cable and two-cable systems are summarized in Fig. 12.

Based upon the results of this investigation, together with previous works,[3-10] it appears that the two-cable tandem suspension system offers a satisfactory method of transporting the standard cargo container throughout the speed range of most present-day cargo helicopters. The system could be enhanced, of course, by incorporating fore and aft hoists to extract loads where cables in excess of 50 ft are required. Also, because of pilot preference for the less complicated single-point suspension system and because of it's structural simplicity, the newly predicted single-cable boundary might well provide an adequate operating envelope for a large number of short-haul application.

The use of a linearized perturbation model, the decoupling of the load and aircraft dynamics, and the assumption that the rotor wake trails the load, limit the applicability of the results obtained here. However, the stability derivatives obtained[1] do indicate that a linearized region, although small, does exist. In addition, for slung loads which are considerably smaller than the weight of the helicopter, for example when the 70,000-lb CH-47 helicopter tows a 4,000- to 10,000-lb load, the dynamic coupling should be small. Finally, except for the case of short cables and very low speeds, the rotor wake does trail the slung load.[13] Thus, the results are applicable in many practical situations and should be of significance for those engaged in slung-load operations. While a comparison of the results obtained here with limited flight-test data shows excellent agreement, further flight testing with a full-size container should be performed to verify the predicted stability boundaries for both the single- and two-cable arrangements.

References

[1] Poli, C. and Cromack, D., "Dynamics of Slung Bodies Using a Single-Point Suspension System," *Journal of Aircraft*, Vol. 10, Feb. 1973, pp. 80-86.

[2] Etkin, B. and Mackworth, J. C., "Aerodynamic Instability of Non-Lifting Bodies Towed Beneath an Aircraft," Institute of Aerophysics, University of Toronto, Toronto, Canada, UTIA TN 65, 1963.

[3] Hutto, A. J., "Qualitative Report on Flight Test of a Two-Point External Load Suspension System", American Helicopter Society, AHS Preprint 473, Jan. 1970.

[4] Gabel, R. and Wilson, G., "Test Approaches to External Sling Load Instabilities," *Proceedings of the American Helicopter Society National Forum*, May 1968.

[5] Szustak, L. and Jenney, D., "Control of Large Crane Helicopters," *Journal of the American Helicopter Society*, Vol. 16, July 1971, pp. 11-22.

[6] Micale, E. and Poli, C., "Dynamics of Slung Bodies Utilizing a Rotating Wheel for Stability," *Journal of Aircraft*, Vol. 10, Dec. 1973, pp. 760-763.

[7] Asseo, S., "Feasibility of Using Active Winch Controllers for Sling-Load Stabilization in Heavy Lift Helicopters," Cornell Aeronautical Laboratory Report No. TG-3083-J, Aug. 1971.

[8] Asseo, S. and Erickson, Jr., "The Control Requirements for the Stabilization of Externally Slung Loads in Heavy Lift Helicopters," Cornell Aeronautical Laboratory Report No. AK-5069-J-1, Dec. 1971.

[9] Asseo, S. and Whitbeck, R., "Control Requirements for Sling-Load Stablization in Heavy Lift Helicopters," *Journal of the American Helicopter Society*, Vol. 18, July 1973, pp. 23-31.

[10] Sheldon, D. F., "An Appreciation of the Dynamic Problems Associated with the External Transportation of Loads from a Helicopter-State of Art," presented at the First European Rotorcraft and Powered Lift Aircraft Forum, University of Southampton, England, Sept. 1975.

[11] Feaster, L., "Dynamics of a Slung Load," Ph.D dissertation, University of Massachusetts, Amherst, Mass., June 1975.

[12] Perkins, C., and Hage, R., *Airplane Performance, Stability, and Control*, John Wiley and Sons, Inc., New York, 1949, Chap. 11.

[13] Niemi, E. E., "The Helicopter Flow Field-A Literature Survey," Progress Report for Towed Vechicle Dynamics, U. S. Army Research Office, Durham, Grant DA-ARO-D-31-124-70-665, Aug. 1971.